

A molecular assessment of phylogenetic relationships and lineage accumulation rates within the family Salamandridae (Amphibia, Caudata)

David W. Weisrock^{a,*}, Theodore J. Papenfuss^b, J. Robert Macey^b, Spartak N. Litvinchuk^c, Rosa Polymeni^d, Ismail H. Ugurtas^e, Ermi Zhao^f, Houman Jowkar^g, Allan Larson^a

^a Department of Biology, Box 1137, Washington University, Saint Louis, MO 63130, USA

^b Museum of Vertebrate Zoology, 3101 Valley Life Science Building, University of California, Berkeley, CA 94720, USA

^c Institute of Cytology, Russian Academy of Sciences, Tikhoretsky Pr., 4, 194064 St. Petersburg, Russia

^d Department of Zoology and Marine Biology, Faculty of Biology, School of Science, University of Athens, GR-15784 Panepistimioupolis, Athens, Greece

^e Department of Biology, Uludag University, 16059 Bursa, Turkey

^f Chengdu Institute of Biology, Academia Sinica, Chengdu, Sichuan, China

^g Tehran University, Tehran, Iran

Received 13 January 2006; revised 4 May 2006; accepted 9 May 2006

Available online 19 May 2006

Abstract

We examine phylogenetic relationships among salamanders of the family Salamandridae using approximately 2700 bases of new mtDNA sequence data (the tRNA^{Leu}, ND1, tRNA^{Ile}, tRNA^{Gln}, tRNA^{Met}, ND2, tRNA^{Trp}, tRNA^{Ala}, tRNA^{Asn}, tRNA^{Cys}, tRNA^{Tyr}, and COI genes and the origin for light-strand replication) collected from 96 individuals representing 61 of the 66 recognized salamandrid species and outgroups. Phylogenetic analyses using maximum parsimony and Bayesian analysis are performed on the new data alone and combined with previously reported sequences from other parts of the mitochondrial genome. The basal phylogenetic split is a polytomy of lineages ancestral to (1) the Italian newt *Salamandrina terdigitata*, (2) a strongly supported clade comprising the “true” salamanders (genera *Chioglossa*, *Mertensiella*, *Lyciasalamandra*, and *Salamandra*), and (3) a strongly supported clade comprising all newts except *S. terdigitata*. Strongly supported clades within the true salamanders include monophyly of each genus and grouping *Chioglossa* and *Mertensiella* as the sister taxon to a clade comprising *Lyciasalamandra* and *Salamandra*. Among newts, genera *Echinotriton*, *Pleurodeles*, and *Tylototriton* form a strongly supported clade whose sister taxon comprises the genera *Calotriton*, *Cynops*, *Euproctus*, *Neurergus*, *Notophthalmus*, *Pachytriton*, *Paramesotriton*, *Taricha*, and *Triturus*. Our results strongly support monophyly of all polytypic newt genera except *Paramesotriton* and *Triturus*, which appear paraphyletic, and *Calotriton*, for which only one of the two species is sampled. Other well-supported clades within newts include (1) Asian genera *Cynops*, *Pachytriton*, and *Paramesotriton*, (2) North American genera *Notophthalmus* and *Taricha*, (3) the *Triturus vulgaris* species group, and (4) the *Triturus cristatus* species group; some additional groupings appear strong in Bayesian but not parsimony analyses. Rates of lineage accumulation through time are evaluated using this nearly comprehensive sampling of salamandrid species-level lineages. Rate of lineage accumulation appears constant throughout salamandrid evolutionary history with no obvious fluctuations associated with origins of morphological or ecological novelties.

© 2006 Elsevier Inc. All rights reserved.

Keywords: Lineage accumulation; Mitochondrial DNA; Newt; Salamander; Salamandridae

* Corresponding author. Present address: Department of Biology, University of Kentucky, 101 Morgan Building, Lexington, KY, 40506-0225, USA. Fax: +859 257 1717.

E-mail address: weisrock@uky.edu (D.W. Weisrock).

1. Introduction

The salamander family Salamandridae, comprising 16 genera and 66 recognized species, represents one of the most diverse groups of extant salamanders. Salamandrids have the largest geographic distribution of any salamander family, extending across the holarctic continents of Asia, Europe, and North America with a small and recent expansion into North Africa. The Salamandridae, which contains the traditionally recognized newts (salamanders with rough keratinized skin) and the “true” salamanders (smooth-skinned salamandrids), has diversified in both terrestrial and aquatic environments through a variety of derived feeding morphologies (Özeti and Wake, 1969; Wake and Özeti, 1969), and courtship behaviors (Salthe, 1967). The historical association between these evolutionary derivations and rates of lineage accumulation (Schluter, 2000) remains to be measured. The salamandrid fossil record is sparse, requiring that rates of lineage accumulation be estimated from systematic studies of extant populations.

Molecular phylogenies are an important framework for studying the tempo of lineage diversification (Slowinski and Guyer, 1989; Mooers and Heard, 1997; Nee et al., 1994; Sanderson and Donoghue, 1996). Plotting lineage accumulation as a function of estimated divergence time and integrating this information with null models of the birth and death of lineages (Nee et al., 1992) permit statistical testing of hypotheses of lineage diversification over time (Paradis, 1997; Pybus and Harvey, 2000; Pybus et al., 2002). These phylogenetic approaches have yielded important insight in the tempo of evolutionary diversification in diverse organismal groups including iguanian lizards (Harmon et al., 2003), marine fishes (Ruber and Zardoya, 2005), mosses (Shaw et al., 2003), and plethodontid salamanders (Kozak et al., 2006).

No single phylogenetic study has sampled all salamandrid species. The most complete prior study (Titus and Larson, 1995) used a combination of morphological and mitochondrial DNA (mtDNA) (12S and 16S rDNA and the intervening tRNA^{Val} gene) characters from 18 species. This study provided strong support for monophyly of the Salamandridae and for some intergeneric groupings, which were congruent with molecular phylogenetic results for 10 genera reported by Frost et al. (2006). Monophyly was statistically rejected for the genera *Mertensiella* and *Triturus*. However, there was little support for many basal relationships within the family, particularly for the placement of the monotypic newt genus *Salamandrina*.

Phylogenetic relationships within many salamandrid groups have received considerable attention (e.g. Caccione et al., 1997; Carranza and Amat, 2005; Chan et al., 2001; Lu et al., 2004; Steinfartz et al., 2000, 2002; Veith et al., 2004; Weisrock et al., 2001), yet many species-level relationships require further resolution. Evolution of the genus *Triturus* has been studied extensively (Halliday and Arano, 1991), yet phylogenetic resolution among species remains ambiguous, even with a host of morphological, molecular, and

behavioral data (Giacomo and Balletto, 1988; Macgregor et al., 1990; Rafinski and Arntzen, 1987; Zajc and Arntzen, 1999). Monophyly of the genus *Triturus* was rejected by the mtDNA studies of Titus and Larson (1995), based on two species. However, studies using more comprehensive ingroup sampling, but limited outgroup sampling have found *Triturus* to be either monophyletic or paraphyletic (e.g. Zajc and Arntzen, 1999). Recent studies of the genus *Euproctus* indicate that it is not monophyletic (Caccione et al., 1994, 1997; Carranza and Amat, 2005), and instead may represent two phylogenetically divergent groups, one of which was recently placed in the genus *Calotriton* (Carranza and Amat, 2005). A thorough phylogenetic assessment of these genera and other salamandrid lineages requires comprehensive species-level sampling of the entire family.

We present a nearly comprehensive species-level sampling of the Salamandridae in conjunction with new and previously published mtDNA sequence data to address both the deep phylogenetic relationships among major lineages of salamandrids and the relationships among the more recently derived lineages. The resulting phylogenies are then used to measure the tempo of lineage diversification across the history of the Salamandridae.

2. Materials and methods

2.1. Taxon sampling and data collection

This study used approximately 2700 bases of new mtDNA sequence data collected from 96 individuals including 61 of the 66 recognized salamandrid species and outgroups. Five salamandrid species were not included: *Triturus helveticus*, *Triturus italicus*, *Calotriton arnoldi*, *Cynops cheng-gongensis*, and *Cynops wolterstorffii*. The latter species is considered to be recently extinct (Zhao, 1998). We follow the taxonomic suggestion of Veith and Steinfartz (2004) in placing *Mertensiella luschani* and related species formerly considered subspecies of *M. luschani* in a new genus, *Lyciasalamandra*, based on mtDNA-based statistical support for the nonmonophyly of the previously recognized genus *Mertensiella* (Weisrock et al., 2001) and corroborating allozyme-based genetic evidence (Veith and Steinfartz, 2004).

Sequence data were collected from a contiguous block of genes including the tRNA^{Leu}, ND1, tRNA^{Ile}, tRNA^{Gln}, tRNA^{Met}, ND2, tRNA^{Trp}, tRNA^{Ala}, tRNA^{Asn} genes, the origin for light-strand replication (O_L), and the tRNA^{Cys}, tRNA^{Tyr}, and COI genes (hereafter called the tRNA^{Leu}–COI genic region). All genes included are full-length except for COI, which contained approximately 30 bases of 5' partial sequence. This gene region is similar to the one used in an earlier study of the “true” salamanders (Weisrock et al., 2001), except that it contains approximately 670 additional bases of sequence completing the 5' portion of the ND1 gene and the preceding tRNA^{Leu} gene. These additional sequences were generated for individuals used by Weisrock et al., 2001 and added to their GenBank records. DNA

extraction, PCR, and sequencing methods were performed as in Weisrock et al. (2001) with the exception that most sequencing reactions were performed using a Big-Dye Terminator Ready-Reaction Kit (Perkin-Elmer) and run on either an ABI™ (PE Applied Biosystems, Inc.) 373A automated DNA sequencer or an MJ Research BaseStation.

We also included GenBank and published mtDNA sequence data from two additional gene regions for use in combined phylogenetic analyses with our data. This included a data set of 12S-tRNA^{Val}-16S sequence for 32 ingroup taxa and 5 outgroups (Caccone et al., 1994; Steinfartz et al., 2002; Titus and Larson, 1995; Zajc and Arntzen, 1999) and a data set of Cytochrome *b* sequences for 32 ingroup taxa and 2 outgroups (Alexandrino et al., 2002; Caccone et al., 1994; Chan et al., 2001; Chippindale et al., 2001; García-Paris et al., 2003; Hedges et al., 1992; Tan and Wake, 1995). Sequences in the 12S-tRNA^{Val}-16S region range from approximately 300–1000 bp in length. Sequences in the Cytochrome *b* data set range from approximately 380 to 700 bp in length. See Appendix A for more detail regarding these sequences. Additional mitochondrial regions are available in GenBank but provide insufficient sampling for this study. All new mtDNA sequences have been placed in GenBank with accession numbers listed in Table 1. An alignment of the new mtDNA sequence data is deposited in TreeBASE under Accession No. S1513.

2.2. Phylogenetic analysis

Alignment of the mtDNA sequences was performed manually using amino-acid sequence translations for protein-coding genes and secondary-structural models for tRNA genes (Kumazawa and Nishida, 1993). Length-variable regions whose alignment was ambiguous, including many loop regions of tRNAs and much of the origin for light-strand replication (O_L), were excluded from phylogenetic analyses.

Phylogenetic trees were generated under both parsimony and Bayesian criteria in the analysis of our new data set as well as in combined analyses with previously published sequence data. Parsimony analysis was performed using PAUP* v4.0 (Swofford, 2002). A heuristic search option with 100 random-addition replicates was used with equal weighting of all characters and TBR branch swapping. To assess support for branches in parsimony trees, bootstrap percentages (BPs) were calculated using 1000 bootstrap replicates with 100 random additions per replicate, and decay indices were calculated using constraint trees generated in TreeRot v2 (Sorenson, 1999) and analyzed in PAUP*. Bayesian phylogenetic analysis was performed using the parallel-processor version of MrBayes v3.04 (Altekar et al., 2004). Bayesian analysis of the new mtDNA sequence data was performed by treating all sequence data as a single data partition and by using a three-partition format: ND1, ND2+COI, and tRNA sequence data. Combined analysis of the new data and previously published sequences used

five data partitions: ND1, ND2+COI, Cytochrome *b*, 12S+16S, and tRNA sequence data. All analyses used four Markov chains with the temperature profile at the default setting of 0.2. The best-fit evolutionary model used was determined using the Akaike Information Criterion as implemented in MODELTEST v3.06 (Posada and Crandall, 1998). Flat Dirichlet priors were used for the six general time-reversible (GTR) substitution-rate parameters and for all base-frequency parameters. A flat Beta prior was used in estimating the transition/transversion substitution-rate parameter. Uniform priors were used for the gamma shape parameter and the proportion of invariant sites parameter. Unconstrained, uniform priors were used for topology and branch-length estimation. A molecular clock was not enforced. Two million generations were run with a sample taken every 1000th generation for a total of 2000 trees. The program TRACER (Rambaut and Drummond, 2003) was used to determine when the log likelihood ($\ln L$) of sampled trees reached a stationary distribution. In all Bayesian analyses, the posterior distribution was reached within 50,000 generations; the first 1 million generations were discarded as “burn in.” Sampled trees from the posterior distribution were parsed with MrBayes to construct a phylogram based upon mean branch lengths and to calculate the posterior probabilities (PPs) of all branches using a majority-rule consensus approach. To account for the possibility that individual analyses may not be converging upon the optimal posterior distribution, two additional independent runs were performed for each data set using identical conditions. Likelihood values, tree topology, branch lengths, and posterior probabilities were compared across the replicated runs to verify that similar results were being achieved.

Alternative phylogenetic topologies were tested using the Templeton Test (Templeton, 1983) and the Shimodaira and Hasegawa (SH) test using 1000 RELL bootstrap replicates (Goldman et al., 2000; Shimodaira and Hasegawa, 1999), both implemented in PAUP* v4.0. To perform the SH tests, a maximum-likelihood tree was found in an unconstrained analysis treating the entire data set as a single partition and using the best-fit model of evolution. Model parameter estimates were set using mean parameter estimates from an unpartitioned Bayesian phylogenetic analysis. The unconstrained ML tree was compared to an ML tree favoring a particular topological constraint. To expedite the likelihood search for constrained ML trees, we preserved branches in the constraint tree that had Bayesian posterior probabilities ≥ 0.95 , were present in the parsimony tree, and were invariant between the alternative hypotheses being tested. The search strategy for finding alternative phylogenetic hypotheses for use in Templeton tests followed a similar methodology.

2.3. Diversification analyses

To obtain ultrametric trees for use in diversification analyses, trees from the Bayesian posterior distribution

Table 1

Taxon sampling for all outgroup and ingroup samples used in this study

Taxon	Specimen Accession No.	GenBank Accession No.	Locality description
<i>Necturus alabamensis</i>	MVZ187705	DQ517763	Walton County, Florida, USA
<i>Ambystoma tigrinum</i>	MVZ187202	DQ517764	Oakland County, Michigan, USA
<i>Eurycea wilderae</i>	KHK188.8	DQ517762	Macon County, North Carolina, USA
<i>Phaeognathus hubrichti</i>	MVZ173507	DQ517761	Butler County, Alabama, USA
<i>Dicamptodon tenebrosus</i>	MVZ187929	DQ517765	Trinity County, California, USA
<i>Calotriton asper</i>	TP-MVZ	DQ517766	Pyrenees Mountains, Spain
<i>Chioglossa lusitanica</i>	MVZ230958	DQ517767	San Martin de Luina, Asturias, Spain
<i>Cynops cyanurus</i>	MVZ219759	DQ517768	Chuxiong, Yunnan Province, China
<i>Cynops ensicauda</i>	MVZ238580	DQ517769	Tokashiki-jima, Ryukyu Islands, Japan
<i>Cynops orientalis</i>	MVZ231158	DQ517771	Fujian Province, China
<i>Cynops orientalis</i>	MVZ230344	DQ517770	Laohe Shan, Hangzhao He, Hangzhou, Zhejiang Province, China
<i>Cynops orphicus</i>	MVZ241427	DQ517772	Tian Chi Lake, Chaoan County, Guangdong Province, China
<i>Cynops pyrrhogaster</i>	TP-MVZ	DQ517773	Japan
<i>Echinotriton andersoni</i>	MVZ232187	DQ517774	Tokunoshima, Kagoshima Prefecture, Kyushu, Japan
<i>Echinotriton chinhaiensis</i>	TP-MVZ	DQ517775	Beilun Forest Park, Ningbo, Zhejiang Province, China
<i>Euproctus montanus</i>	MNHN1978.584	DQ517776	Corsica Island, France
<i>Euproctus platycephalus</i>	MVZ241303	DQ517777	Sette Fratelli, Sardegna Region, Sardinia, Italy
<i>Lyciasalamandra antalyana</i>	MVZ230190	DQ517778	Hurma Köyü, Antalya Province, Turkey
<i>Lyciasalamandra atifi</i>	MVZ230197	DQ517779	Fersin Köyü, Antalya Province, Turkey
<i>Lyciasalamandra billae</i>	MVZ230184	DQ517781	Bnyk Calticak Beach, Antalya Province, Turkey
<i>Lyciasalamandra fazilae</i>	MVZ230159	DQ517782	Domuz Adasi, Fethiye Bay, Mugla Province, Turkey
<i>Lyciasalamandra flavimembris</i>	MVZ230148	DQ517784	Cicekli Köyü, Mugla Province, Turkey
<i>Lyciasalamandra helverseni</i>	MVZ233325	DQ517785	Karpathos Island, Greece
<i>Lyciasalamandra l. luschani</i>	MVZ230165	DQ517786	Dodurga Köyü, Mugla Province, Turkey
<i>Lyciasalamandra luschani basoglu</i>	MVZ230171	DQ517780	Nandarlar Köyü, Antalya Province, Turkey
<i>Lyciasalamandra luschani finikensis</i>	MVZ230177	DQ517783	Finike, Antalya Province, Turkey
<i>Mertensiella c. caucasica</i>	MVZ218721	DQ517787	~10 km SSE Borzhomi, Georgia
<i>Neurergus crocatus</i>	MVZ236763	DQ517788	Beytussebap, Sirnak Province, Turkey
<i>Neurergus kaiseri</i>	MVZ234209	DQ517789	15 km NNW (airline) Chalat, Khuzestan Province, Iran
<i>Neurergus microspilotus</i>	MVZ236826	DQ517790	Najar Darreh, 9 km NW Paveh, Kermanshah Province, Iran
<i>Neurergus s. strauchii</i>	MVZ236768	DQ517791	Yolazi Village, 3 km SW Bitlis, Bitlis Province, Turkey
<i>Neurergus strauchii barani</i>	MVZ236774	DQ517792	Kubbe Mountain, Malatya Province, Turkey
<i>Notophthalmus meridionalis</i>	MVZ250846	DQ517793	Brownsville, Texas, USA
<i>Notophthalmus perstriatus</i>	TP-MVZ	DQ517794	Ocala National Forest, Putnam County, Florida, USA
<i>Notophthalmus v. viridescens</i>	MVZ230959	DQ517795	St. Charles County, Missouri, USA
<i>Pachytriton brevipes</i>	TP-MVZ	DQ517796	Jiulianshan, Quannan county, Jiangxi Province, China
<i>Pachytriton brevipes</i>	MVZ2311167	DQ517797	Qi-Li-Yang, Dai Yun village, Dehua County, Fujian Province, China
<i>Pachytriton labiatum</i>	CAS194298	DQ517798	Jiaxing Prefecture, Zhejiang Province, China
<i>Paramesotriton caudopunctatus</i>	MVZ236250	DQ517799	Leigongshan, Leishan County, Guizhou, China
<i>Paramesotriton chinensis</i>	MVZ230360	DQ517800	Si Hai Shan, Yong Jia County, Zhejiang Province, China
<i>Paramesotriton chinensis</i>	MVZ230616	DQ517801	Mt. Yao, Dayao Shan, Guangxi Province, China
<i>Paramesotriton deloustali</i>	MVZ223627	DQ517802	Tam Dao, Vinh Phu Province, Vietnam
<i>Paramesotriton fuzhongensis</i>	MVZ230363	DQ517803	Mt. Laoxi, Xiling, Guangxi, China
<i>Paramesotriton guanxiensis</i>	MVZ220905	DQ517804	Linming County, Guangxi Zhuang Autonomous Region, China
<i>Paramesotriton hongkongensis</i>	MVZ230365	DQ517807	Ho Chung Valley, New Territories, Hong Kong, China
<i>Paramesotriton hongkongensis</i>	MVZ230367	DQ517805	Violet Hill, Hong Kong Island, Hong Kong, China
<i>Paramesotriton hongkongensis</i>	MVZ230369	DQ517806	Sunset Peak, Lantau Island, Hong Kong, China
<i>Paramesotriton laoensis</i>	FMNH255452	DQ517808	Ban Nyot Phae, Phoukhout District, Khouang Province, Laos
<i>Paramesotriton sp.</i>	ROM35433	DQ517810	Cao Bang Province, Quang Thanh, Vietnam
<i>Paramesotriton sp.</i>	FMNH259125	DQ517809	Bac Kan Province, Vietnam
<i>Paramesotriton sp.</i>	TP-MVZ	DQ517811	Zhongshan, Guangdong Province, China
<i>Pleurodeles poireti</i>	MVZ235670	DQ517812	2 km S Fernana, Jendouba Governorate, Tunisia
<i>Pleurodeles waltl</i>	MVZ162384	DQ517813	5.5 km SE Rabat, Rabat Province, Morocco
<i>Pleurodeles waltl</i>	MVZ186112	DQ517811	2.5 km E Puerto Real, Cadiz Province, Spain
<i>Salamandra algira</i>	MNCN41040	DQ517815	2 km N Thaleta Tagramt, Morocco
<i>Salamandra a. atra</i>	TP-MVZ	DQ517816	Linthal, Kanton Glarus, Switzerland
<i>Salamandra atra aurorae</i>	TP-MVZ	DQ517817	Val d'Assa, Bossco del Dosso, Vicenza, Italy
<i>Salamandra corsica</i>	TP-MVZ	DQ517818	Forêt de l'Ospedale, Corsica Island, France
<i>Salamandra i. infraimmaculata</i>	MVZ230199	DQ517819	Harbiye, Hatay Province, Turkey
<i>Salamandra infraimmaculata semenovi</i>	MVZ236839	DQ517822	3 km N Marivan, Kordestan Province, Iran
<i>Salamandra lanzai</i>	TP-MVZ	DQ517820	Sorgente del Po, Italy
<i>Salamandra salamandra longirostris</i>	MVZ186046	DQ517821	Cadiz, Andalusia, Spain

(continued on next page)

Table 1 (continued)

Taxon	Specimen Accession No.	GenBank Accession No.	Locality description
<i>Salamandrina terdigitata</i>	MVZ178849	DQ517823	Cardoso, Stazzemese, Lucca Province, Toscana Region, Italy
<i>Taricha g. granulosa</i>	KU219725	DQ517824	Camp Kilowan, Polk County, Oregon, USA
<i>Taricha g. granulosa</i>	MVZ173374	DQ517825	Tehama County, California, USA
<i>Taricha rivularis</i>	MVZ158853	DQ517828	Mendocino County, California, USA
<i>Taricha t. torosa</i>	MVZ230652	DQ517826	0.6 mi NE (by road) Briceberg, Mariposa County, California, USA
<i>Taricha t. torosa</i>	MVZ230468	DQ517827	Corral Hollow Rd., San Joaquin County, California, USA
<i>Triturus a. alpestris</i>	ZISP7573	DQ517829	Sukhodol, Opolian Highland, Lvov Province, Ukraine
<i>Triturus alpestris cyreni</i>	TP-MVZ	DQ517830	Cantabria Province, Lloroza, Spain
<i>Triturus boscai</i>	TP-MVZ	DQ517831	Leon Province, Tabuyo, Spain
<i>Triturus c. carnifex</i>	ZISP7565	DQ517832	Venice, Italy
<i>Triturus carnifex macedonicus</i>	ZISP7564	DQ517833	Donja Locanj, Montenegro
<i>Triturus cristatus</i>	ZISP7566	DQ517834	Chur, Udmurtia, Volga River Basin, Russia
<i>Triturus d. dobrogicus</i>	ZISP7567	DQ517835	Vilkovo, Danube River Delta, Odessa Province, Ukraine
<i>Triturus dobrogicus macrosomus</i>	ZISP7568	DQ517836	Minai, Transcarpathian Province, Ukraine
<i>Triturus k. karelinii</i>	CAS182918	DQ517837	Talysh Mountains southeast Azerbaijan
<i>Triturus k. karelinii</i>	MVZ218687	DQ517838	Tbilisi, Georgia
<i>Triturus marmoratus</i>	MVZ191887	DQ517839	Barcelona Province, Catalonia, Spain
<i>Triturus marmoratus</i>	TP-MVZ	DQ517840	Alava Province, Arrillor, Spain
<i>Triturus montandoni</i>	ZISP7571	DQ517842	Sukhodol, Opolian Highland, Lvov Province, Ukraine
<i>Triturus pygmaeus</i>	TP-MVZ	DQ517843	Toledo Province, Pelahustan, Spain
<i>Triturus vittatus ophryticus</i>	MVZ219525	DQ517844	55 km ENE Dagomys, Krasnodar Territory, Russia
<i>Triturus vittatus ophryticus</i>	ZISP5664	DQ517845	Psebai, Krasnodar Territory, Russia
<i>Triturus v. vulgaris</i>	TP-MVZ	DQ517841	Kagul (= Cahul), Cahul Province, Moldavia
<i>Triturus v. vulgaris</i>	TP-MVZ	DQ517848	Dätwil, Kanton Zurich, Switzerland
<i>Triturus vulgaris lantzi</i> (1)	CAS182922	DQ517847	Adler, Krasnodar Territory, Russia
<i>Triturus vulgaris lantzi</i> (2)	ZISP7572	DQ517846	Stavropol, northwest Caucasus Mountains, Russia
<i>Tylotriton asperrimus</i>	TP-MVZ	DQ517849	23 km E Libo, Guizhou Province, China
<i>Tylotriton hainanensis</i>	MVZ230352	DQ517850	12 km NE Jianfengling, Hainan Province, China
<i>Tylotriton kweichowensis</i>	MVZ230371	DQ517851	Daquan County, Yunnan Province, China
<i>Tylotriton shanjing</i>	MVZ219763	DQ517852	Jingdong Yunnan Province, China
<i>Tylotriton taliangensis</i>	CAS195126	DQ517853	Liangsha Yizu Autonomous Prefecture, Sichuan Province, China
<i>Tylotriton verrucosus</i>	TP-MVZ	DQ517854	Nepal
<i>Tylotriton vietnamensis</i>	ROM35330	DQ517856	Quang Thnh, Cao Bang Province, Vietnam
<i>Tylotriton wenxianensis</i>	MVZ236632	DQ517855	Bazi Village, Pingwu County, Sichuan Province, China

Museum abbreviations are as follows: CAS, California Academy of Sciences (San Francisco, USA); FMNH, Field Museum of Natural History (Chicago, USA); KU, University of Kansas, Museum of Natural History (Lawrence, KS, USA); MNCN, Museo Nacional de Ciencias Naturales (Madrid, Spain); MNHM, Museum National d'Histoire Naturelle, (Paris, France); MVZ, Museum of Vertebrate Zoology (Berkeley, USA); ROM, Royal Ontario Museum (Ontario, Canada); ZISP, Zoological Institute of Russian Academy of Sciences (St. Petersburg, Russia). Specimen accession numbers marked as TP-MVZ are to be catalogued in the Museum of Vertebrate Zoology. The KHK sample is from the personal collection of K. Kozak.

were subjected to lineage rate smoothing using a penalized likelihood procedure (Sanderson, 2002a) in the program r8s v1.7 (Sanderson, 2002b). Because current implementation of the Bayesian tree-search algorithm may be prone to overresolution in areas of a tree better represented by a polytomy (Lewis et al., 2005), and because overresolution of branching structure may influence the results of our diversification analyses, we also generated a maximum-likelihood (ML) tree for our diversification analyses using the program PHYML v2.4.4 (Guindon and Gascuel, 2003). A neighbor-joining tree was used as the starting tree in the PHYML analysis, and substitution-parameter estimates were set to the average of the Bayesian posterior distribution. Outgroup taxa were pruned from the Bayesian and ML trees as well as nine ingroup sequences that were shallowly diverged (<1% pairwise sequence divergence) from additional conspecific samples. Rate smoothing was performed using the truncated Newton method and a smoothing value of 10 (indicated as optimal through a cross-validation procedure) in r8s (Sanderson, 2002a).

To obtain a visual perspective of the rate of lineage accumulation over time, we constructed lineage-through-time (LTT) plots (Nee et al., 1992) for 10 trees sampled from the posterior distribution (trees 1, 101, 201, 302, 401, 501, 601, 700, 801, and 900) and for the ML tree using the program LTT (written by L. Harmon). For each of these trees, we quantified the LTT patterns using the γ statistic (Pybus and Harvey, 2000; Pybus et al., 2002). Trees exhibiting increased speciation rates during all or a portion of their history (or decreased extinction rates) are expected to produce concave LTT plots and a $\gamma > 0$, whereas trees that exhibit a decrease in speciation rates (or increased extinction rates) are expected to produce a convex LTT plot and a $\gamma < 0$. Incomplete lineage sampling is expected to omit nodes towards the tips of the tree, and can influence the overall LTT and γ results (Pybus et al., 2002; Harmon et al., 2003). Therefore, we also investigated patterns of lineage accumulation in the early evolutionary history of the Salamandridae by calculating γ for the first two-thirds of each tree (starting from the deepest node to a cumulative branch length of 0.67).

Gamma statistics were used in a constant-rate (CR) test (Pybus and Harvey, 2000) to assess whether the rates of lineage accumulation over time have changed. Because we have nearly complete species sampling for the family, the CR test is appropriate without having to perform a Monte Carlo simulation to account for missing lineages. Under the CR test, a constant-rates model of lineage accumulation can be rejected when $\gamma < -1.645$ (Pybus et al., 2002). The CR test assumes that lineage accumulation occurs equally across the phylogeny; therefore, we used the relative-cladogenesis statistic (P_k) as implemented in the program EndEpi v1.0.1 (Rambaut et al., 1997) to identify ancestral branches that significantly exceed expected rates of lineage accumulation. This test calculates the probability (P_k) that a particular lineage at time t will have k tips given the total number of tips at time 0 (the present).

3. Results

3.1. New *tRNA^{Leu}-COI* salamandrid phylogeny

The sequence alignment of the *tRNA^{Leu}-COI* genic region after exclusion of ambiguously aligned characters contains 2607 characters for phylogenetic analysis (1705 variable, 1483 parsimony informative). The Akaike Information Criterion chooses the GTR model for the total data set with a proportion of sites being invariable (I) and rate heterogeneity across sites (Γ). The individual *ND1* and *ND2 + COI* data partitions are also favored by the GTR + I + Γ model. The *tRNA* partition was found to be best fit to an HKY + I + Γ model. Bayesian analysis of the unpartitioned *tRNA^{Leu}-COI* data produces a posterior distribution with an average lnL of $-62,785.3$. A Bayesian analysis treating the *ND1*, *ND2 + COI*, and *tRNA* data as separate partitions produces a posterior distribution with an average lnL of $-62,676.71$. Mean model parameter estimates of each data partition calculated from the Bayesian posterior distribution are presented in Table 3. The unpartitioned and tri-partitioned Bayesian analyses produce similar topologies, and a generalized partitioned Bayesian consensus phylogram is presented (Fig. 1). Parsimony analysis produces 14 trees of 14,198 steps in length whose strict consensus tree (Fig. 2) is topologically very similar to the partitioned Bayesian tree. The resolution and relationships of major clades between the two trees are nearly identical except for the placement of *Salamandrina terdigitata*, which

is the sister lineage to the “true” salamanders in the Bayesian consensus tree but the sister lineage to a clade containing all remaining newts in the parsimony consensus tree. The partitioned Bayesian analysis finds strong support for the clade containing *Salamandrina* and the “true” salamanders (PP=0.95); however this support decreases in the unpartitioned analysis (PP=0.84). Parsimony analysis poorly supports monophyly of all newts (BP < 50%). SH and Templeton tests of alternative phylogenetic relationships regarding the placement of *Salamandrina* were not significant (Table 2). Results among and within major salamandrid clades were highly congruent between the Bayesian and Parsimony analyses. Partitioned Bayesian consensus phylograms for these clades are presented in Figs. 3 and 4, with posterior probabilities and parsimony bootstrap values mapped to individual branches.

3.2. Combined mtDNA phylogeny

Addition of Cytochrome *b* and 12S-*tRNA^{Val}-16S* mtDNA sequence from GenBank produced a combined character matrix of 4529 nucleotides of which 4134 were included in analyses (2405 variable; 2024 parsimony informative). The *Cytochrome b* and *12S + 16S* data sets each specify a GTR + I + Γ model of evolution. An expanded *tRNA* data set including *tRNA^{Val}* favors the HKY + I + Γ model. Bayesian analysis of a five-partition data set (*ND1*, *ND2 + COI*, *tRNAs*, *Cytochrome b*, and *12S + 16S* rDNAs) produces a posterior distribution with an average lnL of $-74,464.94$. Parsimony analysis of the combined data gives a single tree of 16,692 steps in length. Inclusion of these extra data does little to change the branching structure of the *tRNA^{Leu}-COI*-based analyses, nor does it improve branch support for some important relationships. For example, the combined data Bayesian tree places *Salamandrina* as the sister lineage to a clade of “true” salamanders with a PP of 0.72, which is lower than the PP for this relationship in the partitioned Bayesian analysis of the *tRNA^{Leu}-COI* data. Parsimony analysis of the combined data again places *Salamandrina* as the sister lineage to all remaining newts with a bootstrap of 70%.

3.3. Analysis of lineage accumulation

The relative cladogenesis statistic does not reject the hypothesis of equal rates of lineage accumulation through

Table 2

Tests of alternative hypotheses versus those favored by maximum likelihood (Fig. 2; Shimodaira–Hasegawa test) and maximum parsimony (Fig. 1; Templeton test)

Alternative hypothesis	SH test $\Delta \ln L^a$ (p value)	Templeton test Δ steps ^b (p value)
<i>Salamandrina</i> sister lineage to remaining Newt clade	2.006 ($p = 0.36$)	—
<i>Salamandrina</i> sister lineage to “true” salamander clade	—	6 ($p \leq 0.6188$)
<i>Triturus</i> monophyly	53.973 ($p = 0.003$)	25 ($p \leq 0.1338$)
<i>Calotriton</i> + <i>Euproctus</i> monophyly	63.537 ($p < 0.001$)	27 ($p \leq 0.0686$)

A statistically significant result indicates that the alternative hypothesis as stated is rejected in favor of the topology shown in Fig. 1 or 2 as appropriate.

^a Log likelihood difference for the paired trees being tested.

^b Difference in minimum numbers of mutational steps for the paired trees being tested.

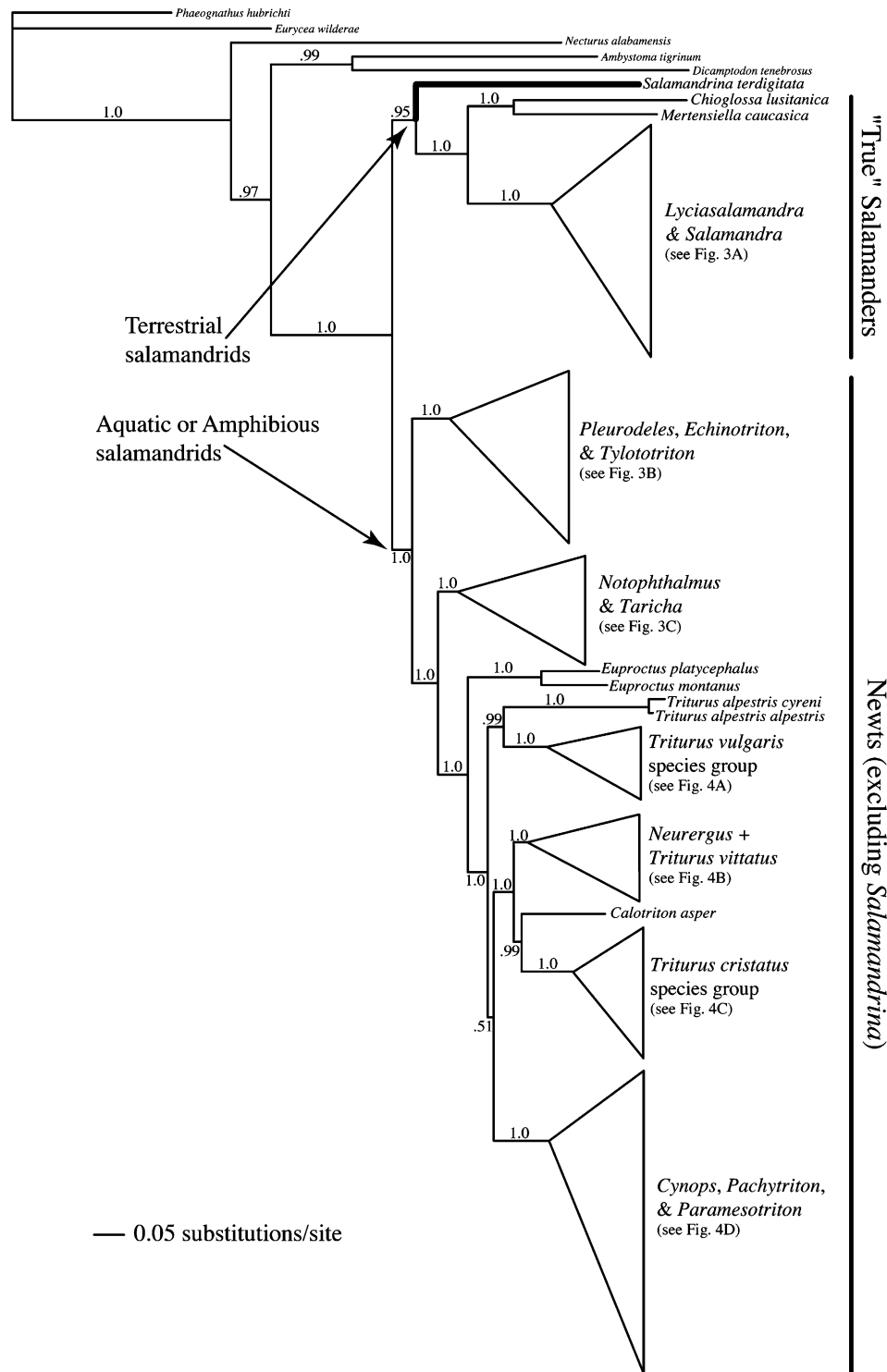


Fig. 1. Bayesian majority-rule consensus phylogram of trees sampled from the posterior distribution of a tri-partitioned analysis of the *tRNA^{Leu}-COI* mtDNA sequence data. Numbers above or below branches are posterior probabilities. Phylogenetic relationships in the unpartitioned analysis did not differ substantially from those of the partitioned analysis. Relationships within major clades are collapsed for easier presentation and are presented in detail in Figs. 3 and 4. The thick black branch leads to *Salamandrina terdigitata*.

time for any branch in the PL-smoothed Bayesian consensus tree and the smoothed ML tree. Lineage-through-time plots for trees sampled from the Bayesian posterior distribution and for the ML tree produce very similar patterns (Fig. 5). All trees exhibit a slightly convex pattern early in

the history of the salamandrid diversification, but the latter portions of the LTT curves do not differ substantially from a pattern expected under a pure-birth model (diagonal dashed line in Fig. 5). Gamma statistics calculated for the total phylogenetic history of each Bayesian tree yield an

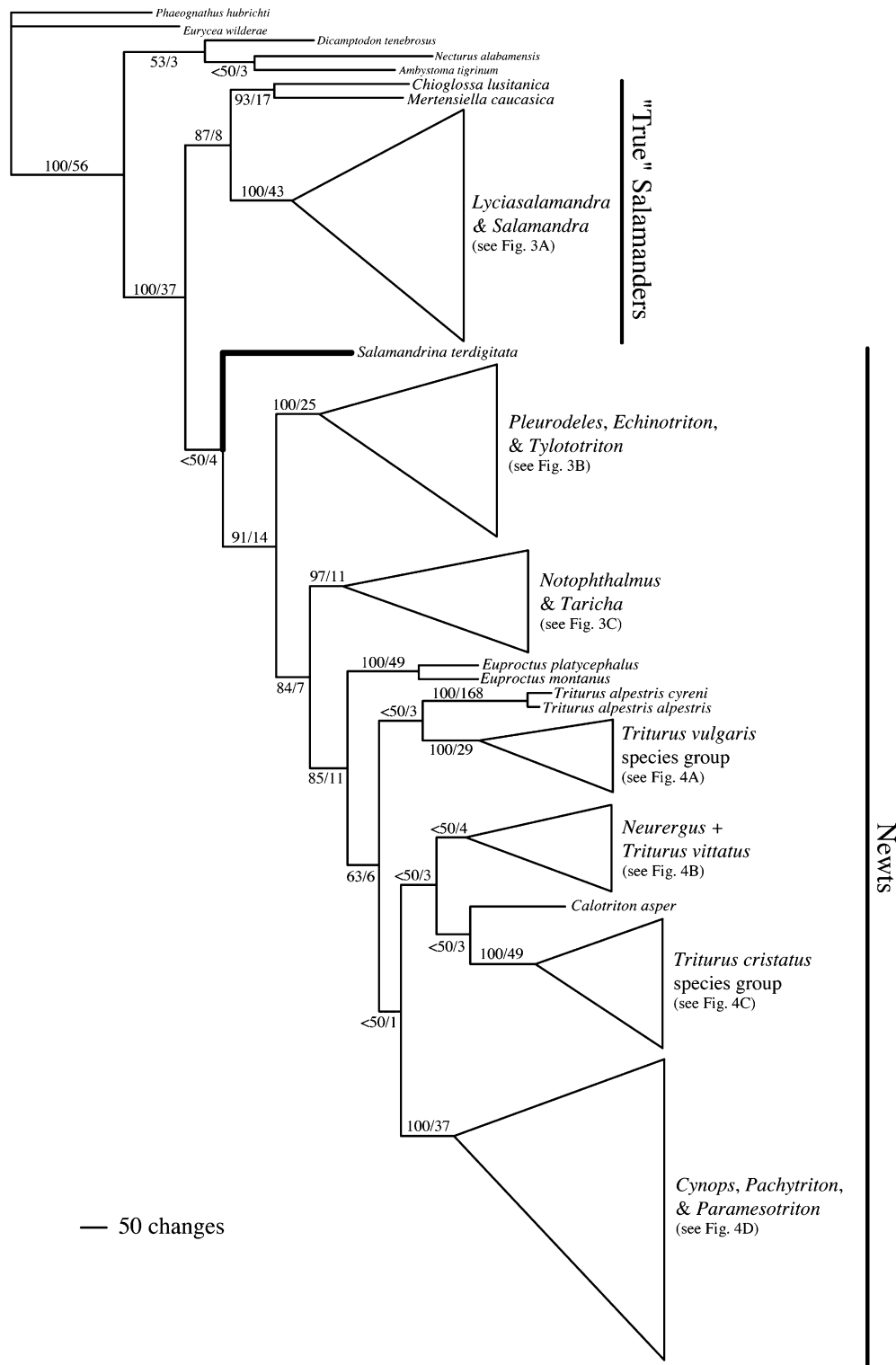


Fig. 2. Consensus parsimony phylogram from analysis of the *tRNA^{Leu}-COI* mtDNA sequence data (2607 aligned positions, 1705 variable, 1483 parsimony informative). Numbers above or below branches represent bootstrap values (before slash) and decay indices (after slash). Relationships within major clades are collapsed for easier presentation and are presented in detail in Figs. 3 and 4. The thick black branch leads to *Salamandrina terdigitata*. The parsimony analysis produces 14 equally most parsimonious trees of 14,198 steps.

average γ of -0.1397 (Table 4; range -0.7317 to 0.4539). The ML tree yields a slightly higher positive γ value of 1.1645 (Table 4). Gamma statistics calculated for the first two-thirds of the phylogenetic history of each Bayesian tree

yield a more negative average γ of -0.8956 (range -1.2302 to -0.5452), and the ML tree is very similar with a γ of -0.7413 (Table 4), congruent with the LTT curves yielding a more convex pattern earlier in salamandrid history.

Table 3
Mean model parameter estimates for each partition of the tRNA^{Leu}-COI genic region calculated from the posterior distribution of the partitioned Bayesian analysis

Model parameter	Total partition	ND1	ND2 + COI	tRNAs
κ	—	—	—	14.165 (1.084)
G ↔ T	1	1	1	—
C ↔ T	5.737 (0.434)	7.788 (1.262)	3.916 (0.437)	—
C ↔ G	0.935 (0.111)	1.335 (0.297)	0.828 (0.148)	—
A ↔ T	0.533 (0.048)	0.7 (0.136)	0.365 (0.052)	—
A ↔ G	13.292 (0.942)	17.157 (2.785)	9.986 (1.147)	—
A ↔ C	0.807 (0.068)	1.078 (0.195)	0.546 (0.068)	—
Freq. A	0.387 (0.006)	0.373 (0.011)	0.4 (0.015)	0.392 (0.014)
Freq. C	0.248 (0.004)	0.254 (0.007)	0.247 (0.007)	0.212 (0.011)
Freq. G	0.067 (0.001)	0.069 (0.002)	0.058 (0.002)	0.151 (0.008)
Freq. T	0.297 (0.005)	0.303 (0.009)	0.295 (0.008)	0.245 (0.011)
Prop. invar.	0.275 (0.011)	0.316 (0.016)	0.24 (0.015)	0.18 (0.026)
α	0.693 (0.017)	0.733 (0.032)	0.802 (0.035)	0.372 (0.023)

Standard deviations for each parameter estimate are given in parentheses.

However, despite the negative γ measured for most trees, no measure of γ rejects a constant rate of lineage accumulation through time.

4. Discussion

4.1. Major salamandrid lineages and their phylogeny

Our results provide the most comprehensive view to date of salamandrid phylogeny. We expand previous phylogenetic assessments of salamandrid phylogeny by generating a data set that includes nearly all recognized species of the family and intraspecific sampling for some species. Analyses of these data provide robust relationships for many of the deep relationships within the family as well as many of the more terminal relationships within major salamandrid clades. We discuss these relationships by first focusing on phylogenetic relationships among the most inclusive clades, and then discussing relationships among the most closely related species.

Our results agree with previous higher-level studies of salamandrid phylogeny (Titus and Larson, 1995) in finding a basal polytomy among three major lineages: (1) the Italian endemic *S. terdigitata*, (2) a lineage ancestral to the mostly European “true” salamanders, and (3) a lineage ancestral to all newts excluding *Salamandrina*. The latter two clades are each strongly supported in both Bayesian and parsimony analyses (Figs. 1 and 2). Monophyly of the “true” salamanders has been supported by previous molecular studies (Veith et al., 1998; Weisrock et al., 2001). Similarly, a newt clade that excluded *Salamandrina* occurred in the trees of Titus and Larson (1995); however, branch support was low (BP = 69–73%). Our results with a nearly comprehensive species-level sampling strongly support a basal split among these three major lineages.

The exact phylogenetic placement of *Salamandrina* remains ambiguous. Partitioned Bayesian analysis of the tRNA^{Leu}-COI mtDNA sequence provides potentially

strong support for grouping *Salamandrina* with the “true” salamanders (PP = 0.95), but support decreases in the unpartitioned analysis of the data (PP = 0.84) and in the combined and partitioned analysis of all mtDNA sequence data (PP = 0.72). Alternatively, parsimony analysis of the tRNA^{Leu}-COI and total mtDNA data sets weakly support the placement of *Salamandrina* as the sister lineage to all remaining newts (BP < 50 and 70%, respectively). The apparently high support for a grouping of *S. terdigitata* with true salamanders in the partitioned Bayesian analysis is potentially an artifact of character weighting coupled with an approximately polytomous branching event located deep in the evolutionary history of the group (see Weisrock et al., 2005, for detailed discussion of this phenomenon in salamander phylogeny).

4.2. Phylogenetics of the “true” salamanders

Relationships within the clade of “true” salamanders support previous molecular studies of this group with a primary phylogenetic split separating a clade containing *ChioGLOSSA* and *Mertensiella* from a clade containing *Lyciasalamandra* and *Salamandra* (Figs. 1 and 2; Veith et al., 1998; Weisrock et al., 2001). *Lyciasalamandra* and *Salamandra* each form well-supported clades. Previous phylogenetic studies within *Salamandra* have not provided robust resolution of dichotomous relationships among species (Barroso and Bogaerts, 2003; García-París et al., 2003; Steinfartz et al., 2000), and our results likewise suggest that the major lineages of *Salamandra* form a polytomy. At the interspecific level, only the grouping of *S. corsica* with *S. atra* appears strong in both parsimony and Bayesian analyses. Species lineages of *Lyciasalamandra* likewise form a polytomy. Weisrock et al. (2001) attributed this polytomy to vicariance caused by tectonic collision between the Arabian plate and the southern edge of Anatolia. Their study included the six species lineages formerly considered subspecies of *M. luschni*; a subsequently recognized species from the Greek islands in the Aegean Sea, *L. helverseni* (Veith and Steinfartz, 2004), differs from the other six species lineages by 10.65% and forms part of this polytomy. Likelihood-ratio tests find the internal branches connecting the seven species lineages of *Lyciasalamandra* not significantly different from zero length (results not shown).

4.3. Phylogenetics of *Echinotriton*, *Pleurodeles*, and *Tylototriton*

Within the large newt clade, our phylogenetic analyses confirm earlier molecular results (Hayashi and Matsui, 1989; Titus and Larson, 1995; Veith et al., 2004) in placing the southern and southeastern Asian genera *Echinotriton* and *Tylototriton* together with the European and North African genus *Pleurodeles* in a strongly supported clade whose sister taxon comprises the remaining newts excluding *Salamandrina* (Figs. 1 and 2). Nearly all branches within this clade are extremely well supported (Fig. 3). Our results

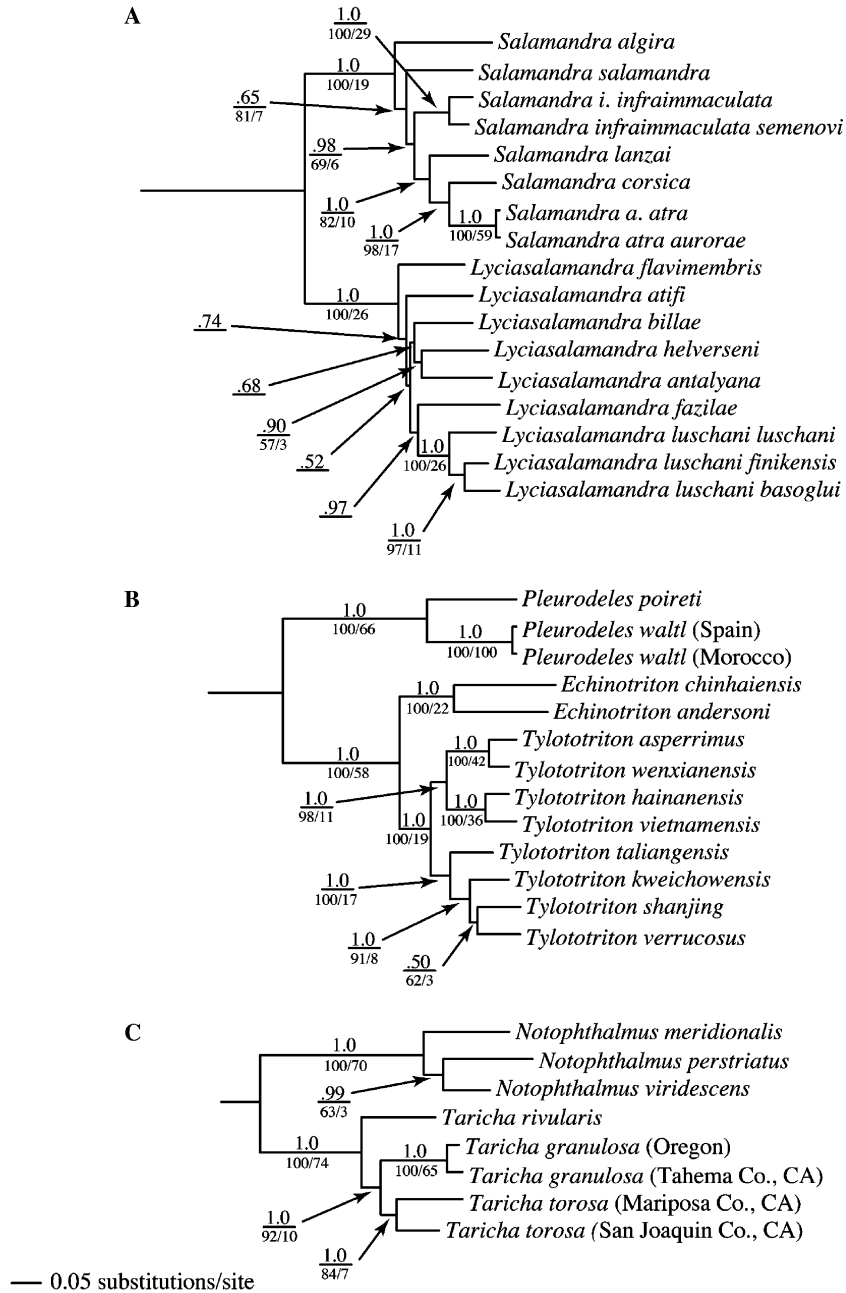


Fig. 3. Phylogenetic relationships for major clades identified in Figs. 1 and 2. This includes relationships for (A) *Lyciasalamandra* and *Salamandra*, (B) *Echinotriton*, *Tylotriton*, and *Pleurodeles*, and (C) *Notophthalmus* and *Taricha*. Branch lengths and topology are from the Bayesian majority-rule consensus phylogram. Numbers above branches are Bayesian posterior probabilities. Numbers below branches are parsimony bootstrap values (before slash) and decay indices (after slash).

confirm the finding of minimal divergence between *P. waltl* haplotypes sampled on either side of the Gibraltar Strait (Veith et al., 2004).

Our results also provide the first assessment of phylogenetic relationships among species of the genera *Echinotriton* and *Tylotriton*. Species of *Echinotriton*, formerly considered part of *Tylotriton*, were described as a new genus because of their distinctness in geographic distribution, morphology, and life history (Nussbaum and Brodie, 1982). Our results support monophyly of *Echinotriton* and

of *Tylotriton* (Fig. 3). Relationships among *Tylotriton* species are extremely well supported except for the relationships among *T. kweichowensis*, *T. shanjing*, and *T. verrucosus*. *Tylotriton shanjing* was formerly part of *T. verrucosus*, but was diagnosed as a distinct species by its unique orange coloration, which distinguishes it from the allopatric brown-colored *T. verrucosus* (Nussbaum et al., 1995). Maximum-likelihood-corrected sequence divergences between *T. shanjing* and *T. verrucosus* haplotypes are nearly 6.2%, indicating considerable genetic

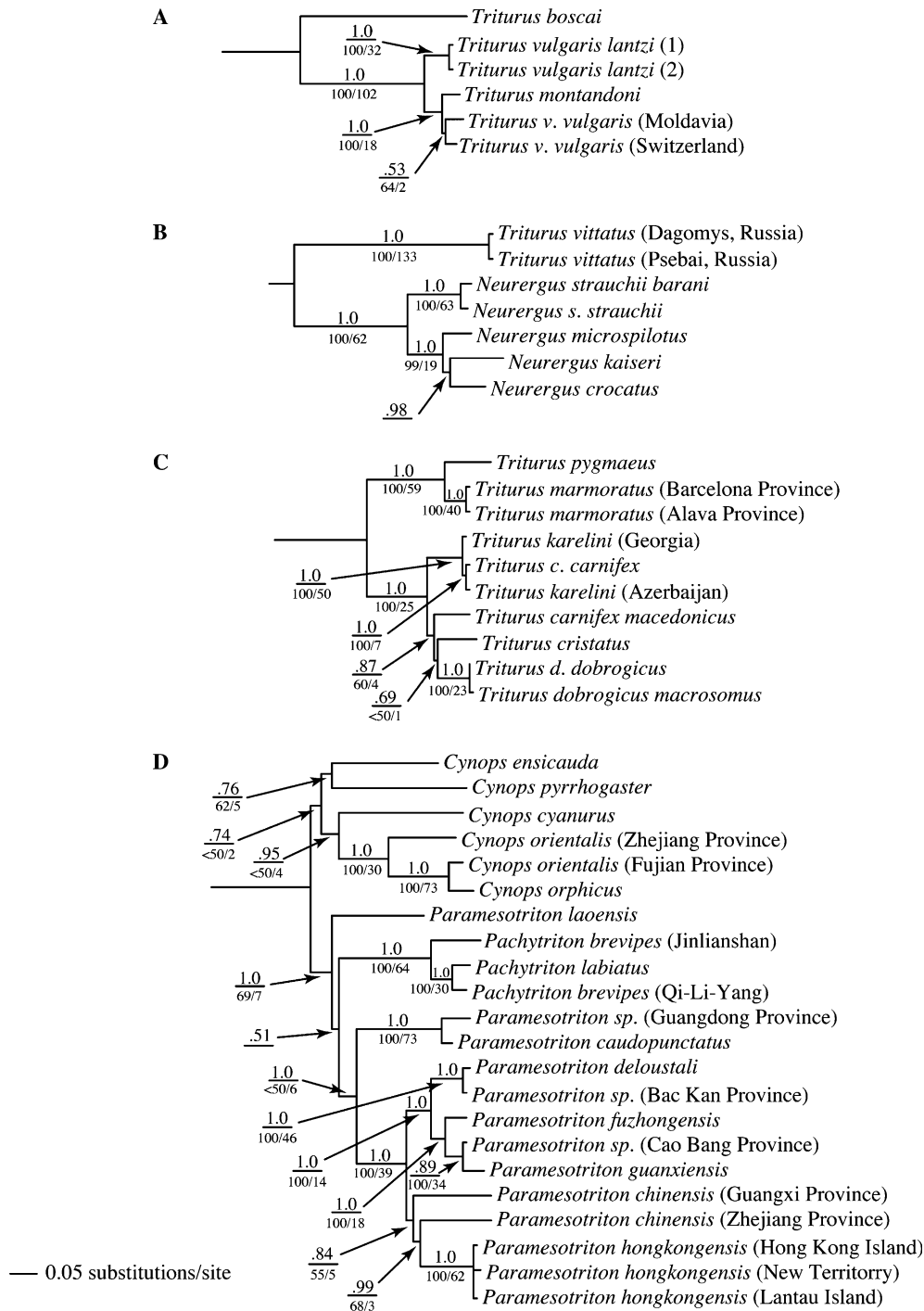


Fig. 4. Phylogenetic relationships for major clades identified in Figs. 1 and 2. This includes relationships for (A) the *Triturus vulgaris* species group, (B) *Neurergus* and *Triturus vittatus*, (C) the *Triturus cristatus* species group, and (D) *Cynops*, *Pachytriton*, and *Paramesotriton*. Branch lengths and topology are from the Bayesian majority-rule consensus phylogram. Numbers above branches are Bayesian posterior probabilities. Numbers below branches are parsimony bootstrap values (before slash) and decay indices (after slash). Branches without a bootstrap value/decay index were not present in the parsimony consensus tree.

divergence. The Chinese Hainan Island species *T. hainanensis* is grouped in a strongly supported clade with the recently described species *Tylotriton vietnamensis* from Vietnam (Böhme et al., 2005). Genetic divergences between these allopatric samples are comparable to those of other *Tylotriton* sister-species pairs.

4.4. Phylogenetics of *Notophthalmus* and *Taricha*

The North American genera *Notophthalmus* and *Taricha* form a clade whose sister group contains all other newts except *Echinotriton*, *Pleurodeles*, *Salamandrina*, and *Tylotriton* (Figs. 1 and 2). The clade comprising *Notophthalmus*

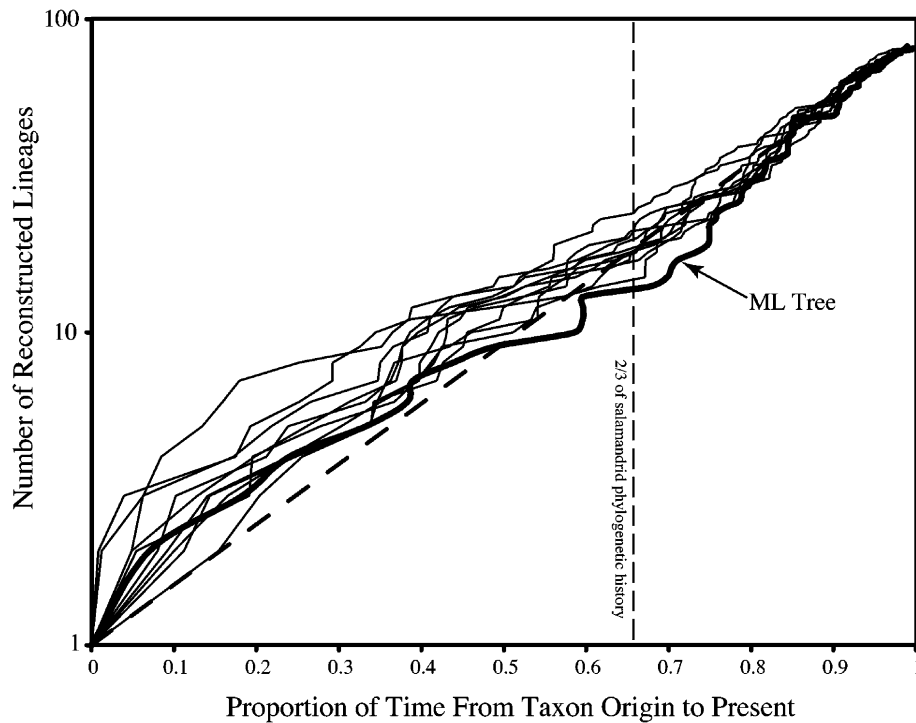


Fig. 5. Lineage-through-time plots for 10 trees sampled from the Bayesian posterior distribution and for the maximum-likelihood tree (thick line). The y-axis (number of reconstructed lineages) is presented in logarithmic format.

and *Taricha* is strongly supported in both the Bayesian and parsimony analyses. Our phylogenetic placement of *Notophthalmus* and *Taricha* is congruent with the allozyme-based phylogeny of Hayashi and Matsui (1989). Relationships among species within *Notophthalmus* and *Taricha* have not previously been explored, although a number of studies have addressed phylogeography within individual species (Gabor and Nice, 2004; Kuchta and Tan, 2005; Reilly, 1990; Tan and Wake, 1995). Within *Notophthalmus*, Bayesian analysis strongly groups *N. perstriatus* and *N. viridescens* as sister species (Fig. 3). Within *Taricha*, *T. granulosa* and *T. torosa* are strongly supported as sister species (Fig. 3).

4.5. Phylogenetics of *Calotriton*, *Euproctus*, *Neurergus*, and *Triturus*

Our results indicate strong support for a large clade containing all species of the genera *Calotriton*, *Cynops*, *Euproctus*, *Neurergus*, *Pachytriton*, *Paramesotriton*, and *Triturus* (Figs. 1 and 2). Within this large clade, the genera *Cynops*, *Pachytriton*, and *Paramesotriton* form a strongly supported clade (discussed below). Monophyly of *Neurergus* is strongly supported (Steinfartz et al., 2002), but its placement as the sister group to a lineage of *Triturus vittatus* contributes to the nonmonophyly of *Triturus*. Molecular phylogenetics of *Triturus* has received considerable attention (Busack et al., 1988; Giacomo and Balleto, 1988; Halliday and Arano, 1991; Macgregor et al., 1990; Zajc and Arntzen, 1999) with some molecular studies indicating that

Table 4

Test for rate constancy of lineage accumulation through evolutionary time

Posterior tree	γ (full tree)	γ (2/3 tree)
Tree 1	-0.3179	-0.9831
Tree 101	-0.5139	-0.6239
Tree 201	0.2209	-0.5452
Tree 302	-0.7317	-0.8437
Tree 401	-0.1910	-0.8419
Tree 501	-0.1776	-1.0221
Tree 601	0.4539	-1.0496
Tree 700	-0.2074	-0.6293
Tree 801	-0.2913	-1.1869
Tree 900	0.3586	-1.2302
Bayesian average	-0.1397	-0.8956
ML tree	1.1675	-0.7413

Gamma statistics (Pybus and Harvey, 2000) for 10 trees sampled from the Bayesian posterior distribution and from the maximum-likelihood tree are shown. The third column covers only the oldest 67% of the tree. Positive values indicate acceleration and negative values deceleration in rates of lineage accumulation through time; none of the values shown differ significantly from zero (= constant rate of lineage accumulation).

it is not monophyletic (Titus and Larson, 1995; Zajc and Arntzen, 1999). Furthermore, molecular (mtDNA and nuclear rDNA) phylogenetic investigations have found that *Calotriton* likewise renders *Triturus* nonmonophyletic (Caccone et al., 1994, 1997; Carranza and Amat, 2005).

Through nearly complete taxon sampling, our results resolve a nonmonophyletic history for *Triturus* (Figs. 1, 2, and 4). We divide *Triturus* species into four main parts: (1) a clade containing all species of the *T. cristatus* species

group (*T. carnifex*, *T. cristatus*, *T. dobrogicus*, *T. karelinii*, *T. marmoratus*, and *T. pygmaeus*); (2) a clade containing the *T. vulgaris* species group (*T. montandoni* and *T. vulgaris*) and *T. boscai*; (3) *T. alpestris*, and (4) *T. vittatus*, whose sister taxon is *Neurergus*.

As in previous studies (Caccone et al., 1994, 1997), the Mediterranean island *Euproctus* species, *E. montanus* (Corsica) and *E. platycephalus* (Sardinia) form a strongly supported clade. This group is the sister taxon to a large and diverse newt clade containing *Calotriton* and *Pachytriton*, *Paramesotriton*, and *Triturus*, although the latter clade receives strong support only in the Bayesian analysis. *Calotriton* is placed as the sister taxon to a clade containing all species of the *T. cristatus* species group. Relationships among the above-described lineages of *Euproctus* and *Triturus* and the *Cynops*–*Pachytriton*–*Paramesotriton* clade are robustly supported in the Bayesian analysis with many branches receiving PPs of 0.99–1.0 (Fig. 1). Parsimony analysis finds a congruent topology, but with lower levels of branch support (Fig. 2). Nonetheless, monophyly of *Triturus* is strongly rejected under the conservative SH test, although not under the Templeton test (Table 2); likewise, a clade comprising *Calotriton* and *Euproctus* is rejected by the SH test although not by the Templeton test (Table 2).

4.6. Phylogenetics of *Cynops*, *Pachytriton*, and *Paramesotriton*

Our results confirm previous molecular studies in grouping *Cynops*, *Pachytriton*, and *Paramesotriton* as a monophyletic group (Chan et al., 2001; Hayashi and Matsui, 1988, 1989; Titus and Larson, 1995). Relationships within this clade have been more difficult to resolve. *Pachytriton* is the only genus whose monophyly receives robust support in our analyses (Fig. 4), consistent with the findings of Chan et al. (2001) that *Pachytriton* species are highly distinct in morphology from *Cynops* and *Paramesotriton*. Using mtDNA sequences from two of the six extant species, Chan et al. (2001) found *Cynops* paraphyletic, with *C. pyrrhogaster* forming the sister lineage to a clade of *Pachytriton* and *Paramesotriton*. Our results, which include sequence data from five of the seven *Cynops* species, are consistent with monophyly of *Cynops* but this grouping is not well supported by either Bayesian or parsimony analyses (Fig. 4).

The genus *Paramesotriton* contains divergent genetic lineages that are not resolved as a monophyletic group (Fig. 4). Nonmonophyly of *Paramesotriton* results from the placement of *Paramesotriton laoensis*, a recently described species from Laos (Stuart and Papenfuss, 2002), as the sister lineage to a well-supported clade containing the genus *Pachytriton* and all remaining species of *Paramesotriton* (Fig. 4). *Paramesotriton laoensis* is morphologically distinct from other *Paramesotriton* species in a number of characters, especially in skin coloring, distribution of warts and glands on the skin, and in having an undifferentiated tongue pad (similar to that of *Pachytriton*) (Stuart and Papenfuss, 2002). It is morphologically similar to other spe-

cies of *Paramesotriton* in its skull morphology and vertebral number (12), which are the primary characters used to place *P. laoensis* in the genus *Paramesotriton*. Our results suggest that these shared characters likely represent symplesiomorphies and that *P. laoensis* should not be placed in the genus *Paramesotriton*. It is a distinct evolutionary lineage with ML-corrected sequence divergences from other species of *Paramesotriton* (avg. = 18.1%) comparable to its divergences from the genera *Pachytriton* (avg. = 17.7%) and *Cynops* (avg. = 20.4%).

The remaining species and samples of *Paramesotriton* are strongly supported as a monophyletic group with a Bayesian PP of 1.0 (Fig. 4), and relationships are similar but not identical to those reconstructed by Lu et al. (2004). Differences between our results and theirs in the exact relationships among *P. deloustali*, *P. fuzhongensis*, and *P. guanxiensis* could represent undetected cryptic lineages in one or more of these species. Our data include some recently collected samples that could not be morphologically assigned to recognized species, but whose mitochondrial haplotypes are close to those of recognized species. Haplotypes from geographically distinct samples of the Chinese newt, *Paramesotriton chinensis*, are divergent and may not form a monophyletic group, indicating that this species may contain cryptic evolutionary lineages.

4.7. Tempo of salamandrid diversification

Our results do not support the hypothesis that the Salamandridae has experienced episodes of unusually rapid lineage accumulation (i.e. radiations). Overall, the LTT patterns and γ statistics are similar among the Bayesian and ML trees, indicating that analytical artifacts of the Bayesian tree search strategy (Lewis et al., 2005) are not biasing our results. Our LTT plots and γ statistics exhibit patterns consistent with a slightly higher rate of lineage accumulation early in salamandrid history. However, the CR test does not reject the null hypothesis of constant rates of lineage accumulation across the recoverable history of the Salamandridae. Furthermore, the relative cladogenesis statistic does not identify any internal branches in the Bayesian consensus tree or ML tree as having produced a disproportionate number of subsequent lineages. It also seems unlikely that our results are artifactual as a function of taxon sampling, given that we include nearly all recognized species. Failure to include cryptic or undiscovered lineage diversity (for example, in the genus *Paramesotriton*) would cause an undersampling of lineages near the tips of the tree, and its correction probably would remove all indications that lineage accumulation might have been disproportionately high early in salamandrid phylogeny.

Our results indicate that the evolution of substantial behavioral, ecological, and morphological character variation in the Salamandridae has not coincided with increased rates of speciation and lineage formation. Much attention has been placed on disparity in trophic morphology in salamandrids, which has been characterized as an important

adaptive factor in the evolution of major salamandrid groups (the terrestrial genera *Chioglossa*, *Lyciasalamandra*, *Mertensiella*, *Salamandra*, and *Salamandrina* vs. the remaining aquatic or amphibious genera) (Özeti and Wake, 1969; Titus and Larson, 1995). The evolution of a hyobranchial feeding morphology for aquatic and amphibious salamandrids is considered a derived condition within the family (Titus and Larson, 1995) and interestingly, this condition characterizes the most species-rich clade in salamandrid phylogeny (Fig. 1). Nonetheless, our phylogenetic hypotheses do not identify an increased rate of lineage accumulation within this clade. This observation, and the documented association between lineage accumulation and vicariance in *Lyciasalamandra* (Weisrock et al., 2001), are consistent with the conclusions of Kozak et al. (2006) that biogeographic factors rather than adaptive changes provide the primary explanations for rates of lineage accumulation in salamanders.

Acknowledgments

We thank M. García-París, K. Kozak, M. Lau, P. Moler, R. Roegner, and B. Stuart for providing valuable samples. We thank L. Harmon for help and assistance with the diversification analyses, J. Kolbe with sequencing assistance, M. Tobias for assistance with parallel computing, and the Washington University Center for Scientific Parallel Computing (<http://harpo.wustl.edu>) for providing computer resources. Collecting permit information for the majority of samples used in this study can be obtained through the museums listed in Table 1. This work was supported by NSF grants DDIG-0105066, RFBR 05-04-48815, and DEB9726064.

Appendix A

Previously published mtDNA sequences used in this study are listed below. When available, sequences are marked with their GenBank accession numbers. Not all *12S-tRNA^{Val}-16S* sequences are accessioned in GenBank. Sequences published by Titus and Larson (1995) and Zajc and Arntzen (1999) are marked with TL95 and ZA99, respectively. *12S-tRNA^{Val}-16S* sequences: *Phaeognathus hubrichti*, TL95; *Eurycea wilderae*, TL95; *Necturus maculosus*, TL95; *Ambystoma tigrinum*, TL95; *Dicamptodon tenebrosus*, TL95; *Chioglossa lusitanica*, TL95; *Cynops ensicauda*, TL95; *Cynops pyrrhogaster*, TL95; *Calotriton asper*, TL95; *Euproctus montanus*, U04696; *Euproctus platycephalus*, U04698; *Mertensiella caucasica*, TL95; *Neurergus crocatus*, AY147246; *Neurergus kaiseri*, AY147250; *Neurergus microspilotus*, AY147248; *Neurergus s. strauchii*, TL95; *Neurergus strauchii barani*, AY147244; *Notophthalmus viridescens*, TL95; *Pachytriton labiatus*, TL95; *Paramesotriton deloustali*, TL95; *Pleurodeles waltl*, TL95; *Salamandra a. atra*, TL95; *Salamandra salamandra*, TL95; *Lyciasalamandra luschani*, TL95; *S. terdigitata*, TL95; *Taricha granulosa*, TL95; *Triturus alpestris*, TL95; *Triturus boscai*, ZA99;

Triturus c. carnifex, U04702; *Triturus cristatus*, ZA99; *Triturus karelinii*, TL95; *Triturus marmoratus*, AY147252; *Triturus montandoni*, ZA99; *Triturus vittatus*, ZA99; *Triturus vulgaris*, U04704; *Tylototriton taliangensis*, TL95; *Tylototriton verrucosus*, TL95. *Cytochrome b* sequences: *Ambystoma tigrinum*, Z11640; *Eurycea wilderae*, AF252379; *Chioglossa lusitanica*, AF329300; *Cynops cyanurus*, AF295682; *Cynops pyrrhogaster*, AF295681; *Calotriton asper*, U55945; *Euproctus montanus*, U55946; *Euproctus platycephalus*, U55947; *Mertensiella caucasica*, AF170013; *Neurergus crocatus*, AY336661; *Notophthalmus perstriatus*, AF380362; *Notophthalmus viridescens*, L22882; *Pachytriton labiatus*, AF295679; *Paramesotriton caudopunctatus*, AF295675; *Paramesotriton deloustali*, AF295671; *Paramesotriton guanxiensis*, AF295673; *Paramesotriton hongkongensis*, AF295677; *Pleurodeles poireti*, AY336644; *Pleurodeles waltl*, U55950; *Salamandra salamandra*, AY336658; *Salamandra algira*, AY247734; *Salamandra a. atra*, AY042786; *Salamandra atra aurorae*, AY042784; *Salamandra lanzai*, AY196284; *Lyciasalamandra luschani*, AF154053; *Taricha granulosa*, AF295683; *Taricha rivularis*, L22713; *Taricha torosa*, L22708; *Triturus c. carnifex*, U55949; *Triturus marmoratus*, AY046081; *Triturus pygmaeus*, AY046082; *Triturus vittatus*, AY336659; *Triturus vulgaris*, U55948; *Tylototriton taliangensis*, AF295684; *Tylototriton verrucosus*, AF295685.

References

- Alexandrino, J., Arntzen, J.W., Ferrand, N., 2002. Nested clade analysis and the genetic evidence for population expansion in the phylogeography of the golden-striped salamander, *Chioglossa lusitanica* (Amphibia: Urodela). *Heredity* 88, 66–74.
- Altekar, G., Dwarkadas, S., Huelsenbeck, J.P., Ronquist, F., 2004. Parallel Metropolis coupled Markov chain Monte Carlo for Bayesian phylogenetic inference. *Bioinformatics* 20, 407–415.
- Barroso, D.D., Bogaerts, S., 2003. A new subspecies of *Salamandra algira* Bedriaga, 1883 from northern Morocco. *Podarcis* 4, 84–100.
- Böhme, W., Schöttler, T., Nguyen, T.Q., Köhler, J., 2005. A new species of salamander, genus *Tylototriton* (Urodela: Salamandridae), from northern Vietnam. *Salamandra* 41, 215–220.
- Busack, S.D., Jericho, B.G., Maxson, L.R., Uzzell, T., 1988. Evolutionary relationships of salamanders in the genus *Triturus*: the view from immunology. *Herpetologica* 44, 307–316.
- Caccone, A., Milinkovitch, M.C., Sbordoni, V., Powell, J.R., 1994. Molecular biogeography: using the Corsica-Sardinia microplate disjunction to calibrate mitochondrial rDNA evolutionary rates in mountain newts. *J. Evol. Biol.* 7, 227–245.
- Caccone, A., Milinkovitch, M.C., Sbordoni, V., Powell, J.R., 1997. Mitochondrial DNA rates and biogeography in European newts (genus *Euproctus*). *Syst. Biol.* 46, 126–144.
- Carranza, S., Amat, F., 2005. Taxonomy, biogeography and evolution of *Euproctus* (Amphibia: Salamandridae), with the resurrection of the genus *Calotriton* and the description of a new endemic species from the Iberian Peninsula. *Zool. J. Linnean Soc.* 145, 555–582.
- Chan, L.M., Zamudio, K.R., Wake, D.B., 2001. Relationships of the salamandrid genera *Paramesotriton*, *Pachytriton*, and *Cynops* based on mitochondrial DNA sequences. *Copeia* 2001, 997–1009.
- Chippindale, P.T., Price, A.H., Wiens, J.J., Hillis, D.M., 2001. Phylogenetic relationships and systematic revision of central Texas hemidactyline plethodontid salamanders. *Herpetol. Monogr.* 14, 1–80.

- Frost, D.R., Grant, T., Faivovich, J., Bain, R.H., Haas, A., Haddad, C.F.B., De Sá, R.O., Channing, A., Wilkinson, M., Donnellan, S.C., Raxworthy, C.J., Campbell, J.A., Blotto, B.L., Moler, P., Drewes, R.C., Nussbaum, R.A., Lynch, J.D., Green, D.M., Wheeler, W.C., 2006. The amphibian tree of life. *Bull. Am. Mus. Nat. Hist.* 297, 1–370.
- Gabor, C.R., Nice, C.C., 2004. Genetic variation among populations of eastern newts, *Notophthalmus viridescens*: a preliminary analysis based on allozymes. *Herpetologica* 60, 373–386.
- García-París, M., Alcobendas, M., Buckley, D., Wake, D.B., 2003. Dispersal of viviparity across contact zones in Iberian populations of fire salamanders (*Salamandra*) inferred from discordance of genetic and morphological traits. *Evolution* 57, 129–143.
- Giacomo, C., Balletto, E., 1988. Phylogeny of the salamandrid genus *Triturus*. *Boll. Zool.* 55, 337–360.
- Goldman, N., Anderson, J.P., Rodrigo, A.G., 2000. Likelihood-based tests of topologies in phylogenetics. *Syst. Biol.* 49, 652–670.
- Guindon, S., Gascuel, O., 2003. A simple, fast, and accurate algorithm to estimate large phylogenies by maximum likelihood. *Syst. Biol.* 52, 696–704.
- Halliday, T., Arano, B., 1991. Resolving the phylogeny of the European newts. *Trends Ecol. Evol.* 6, 113–117.
- Harmon, L.J., Schulte II, J.A., Larson, A., Losos, J.B., 2003. Tempo and mode of evolutionary radiation in iguanian lizards. *Science* 301, 961–964.
- Hayashi, T., Matsui, M., 1988. Biochemical differentiation in Japanese newts, genus *Cynops* (Salamandridae). *Zool. Sci. (Tokyo)* 5, 1121–1136.
- Hayashi, T., Matsui, M., 1989. Preliminary study of phylogeny in the family Salamandridae: allozyme data. In: Matsui, M., Hikida, T., Goris, R.C. (Eds.), *Current Herpetology in East Asia*. The Herpetological Society of Japan, Kyoto, pp. 157–167.
- Hedges, S.B., Bogart, J.P., Maxson, L.R., 1992. Ancestry of unisexual salamanders. *Nature* 356, 708–710.
- Kozak, K.H., Weisrock, D.W., Larson, A., 2006. Rapid lineage accumulation in a non-adaptive radiation: phylogeographic analysis of diversification rates in eastern North American woodland salamanders (genus *Plethodon*). *Proc. R. Soc. Lond. B* 273, 539–546.
- Kuchta, S.R., Tan, A.M., 2005. Isolation by distance and post-glacial range expansion in the rough-skinned newt, *Taricha granulosa*. *Mol. Ecol.* 14, 225–244.
- Kumazawa, Y., Nishida, M., 1993. Sequence evolution of mitochondrial transfer RNA genes and deep-branch animal phylogenetics. *J. Mol. Evol.* 37, 380–398.
- Lewis, P.O., Holder, M.T., Holsinger, K.E., 2005. Polytomies and Bayesian phylogenetic inference. *Syst. Biol.* 54, 241–253.
- Lu, S., Yuan, Z., Pang, J., Yang, D., Yu, F., McGuire, P., Xie, F., Zhang, Y., 2004. Molecular phylogeny of the genus *Paramesotriton* (Caudata: Salamandridae). *Biochem. Genet.* 42, 139–148.
- Macgregor, H.C., Sessions, S.K., Arntzen, J.W., 1990. An integrative analysis of phylogenetic relationships among newts of the genus *Triturus* (family Salamandridae), using comparative biochemistry, cytogenetics and reproductive interactions. *J. Evol. Biol.* 3, 329–373.
- Mooers, A.Ø., Heard, S.B., 1997. Inferring evolutionary process from phylogenetic tree shape. *Q. Rev. Biol.* 72, 31–54.
- Nee, S., Mooers, A.Ø., Harvey, P.H., 1992. Tempo and mode of evolution revealed from molecular phylogenies. *Proc. Natl. Acad. Sci. USA* 89, 8322–8326.
- Nee, S., May, R.M., Harvey, P.H., 1994. The reconstructed evolutionary process. *Philos. Trans. R. Soc. B* 344, 305–311.
- Nussbaum, R.A., Brodie Jr., E.D., 1982. Partitioning of the salamandrid genus *Tylostotriton* Anderson (Amphibia: Caudata) with a description of a new genus. *Herpetologica* 38, 320–332.
- Nussbaum, R.A., Brodie Jr., E.D., Datong, Y., 1995. A taxonomic review of *Tylostotriton verrucosus* Anderson (Amphibia: Caudata: Salamandridae). *Herpetologica* 51, 257–268.
- Özeti, N., Wake, D.B., 1969. The morphology and evolution of the tongue and associated structures in salamanders and newts (Family Salamandridae). *Copeia* 1969, 91–123.
- Paradis, E., 1997. Assessing temporal variations in diversification rates from phylogenies: estimation and hypothesis testing. *Proc. R. Soc. Lond. B* 264, 1141–1147.
- Posada, D., Crandall, K.A., 1998. MODELTEST: testing the model of DNA substitution. *Bioinformatics* 14, 817–818.
- Pybus, O.G., Harvey, P.H., 2000. Testing macroevolutionary models using incomplete molecular phylogenies. *Proc. R. Soc. Lond. B* 267, 2267–2272.
- Pybus, O.G., Rambaut, A., Holmes, E.C., Harvey, P.H., 2002. New inferences from tree shape: numbers of missing taxa and population growth rates. *Syst. Biol.* 51, 881–888.
- Rafinski, J., Arntzen, J.W., 1987. Biochemical systematics of the Old World newts, genus *Triturus*: allozyme data. *Herpetologica* 43, 446–457.
- Rambaut, A., Drummond, A.J., 2003. Tracer v1.0.1. Available from <http://evolve.zoo.ox.ac.uk/>.
- Rambaut, A., Harvey, P.H., Nee, S., 1997. End-Epi: an application for inferring phylogenetic and population dynamical processes from molecular sequences. *Comput. Appl. Biosci.* 13, 303–306.
- Reilly, S.M., 1990. Biochemical systematics and evolution of the eastern North American newts, genus *Notophthalmus* (Caudata: Salamandridae). *Herpetologica* 46, 51–59.
- Ruber, L., Zardoya, R., 2005. Rapid cladogenesis in marine fishes revisited. *Evolution* 59, 1119–1127.
- Salthe, S.N., 1967. Courtship patterns and the phylogeny of the Urodeles. *Copeia* 1967, 100–117.
- Sanderson, M.J., 2002a. Estimating absolute rates of molecular evolution and divergence times: a penalized likelihood approach. *Mol. Biol. Evol.* 19, 101–109.
- Sanderson, M.J., 2002b. r8s, version 1.50. Section of evolution and ecology. University of California, Davis, CA.
- Sanderson, M.J., Donoghue, M.J., 1996. Reconstructing shifts in diversification rates on phylogenetic trees. *Trends Ecol. Evol.* 11, 15–20.
- Schluter, D., 2000. *The Ecology of Adaptive Radiation*. Oxford University Press, Oxford.
- Shaw, A.J., Cox, C.J., Goffinet, B., Buck, W.R., Boles, S.B., 2003. Phylogenetic evidence of a rapid radiation of pleurocarpous mosses (Bryophyta). *Evolution* 57, 2226–2241.
- Shimodaira, H., Hasegawa, M., 1999. Multiple comparisons of log-likelihoods with applications to phylogenetic inference. *Mol. Biol. Evol.* 16, 1114–1116.
- Slowinski, J.B., Guyer, C., 1989. Testing the stochasticity of patterns of organismal diversity: an improved null model. *Am. Nat.* 134, 907–921.
- Sorenson, M.D., 1999. TreeRot, version 2. Boston University, Boston, MA.
- Steinfartz, S., Veith, M., Tautz, D., 2000. Mitochondrial sequence analysis of *Salamandra* taxa suggests old splits of major lineages and postglacial recolonizations of central Europe from distinct source populations of *Salamandra salamandra*. *Mol. Ecol.* 9, 397–410.
- Steinfartz, S., Hwang, U.W., Tautz, D., Öz, M., Veith, M., 2002. Molecular phylogeny of the salamandrid genus *Neurergus*: evidence for an intra-generic switch of reproductive biology. *Amphibia-Reptilia* 23, 419–431.
- Stuart, B.L., Papenfuss, T.J., 2002. A new salamander of the genus *Paramesotriton* (Caudata: Salamandridae) from Laos. *J. Herpetol.* 36, 145–148.
- Swofford, D.L., 2002. PAUP*: Phylogenetic Analysis Using Parsimony (*and Other Methods), version 4. Sinauer Associates, Sunderland, MA.
- Tan, A., Wake, D.B., 1995. mtDNA phylogeography of the California newt, *Taricha torosa* (Caudata, Salamandridae). *Mol. Phylogenet. Evol.* 4, 383–394.
- Templeton, A.R., 1983. Phylogenetic inference from restriction endonuclease cleavage site maps with particular reference to the evolution of humans and the apes. *Evolution* 37, 221–244.
- Titus, T.A., Larson, A., 1995. A molecular phylogenetic perspective on the evolutionary radiation of the salamander family Salamandridae. *Syst. Biol.* 44, 125–151.
- Veith, M., Steinfartz, S., 2004. When non-monophyly results in taxonomic consequences—the case of *Mertensiella* within the Salamandridae (Amphibia: Urodela). *Salamandra* 40, 67–80.
- Veith, M., Steinfartz, S., Zardoya, R., Seitz, A., Meyer, A., 1998. A molecular phylogeny of “true” salamanders (family Salamandridae) and the evolution of terrestriality of reproductive modes. *J. Zool. Syst. Evol. Res.* 36, 7–16.
- Veith, M., Mayer, C., Samraoui, B., Barroso, D.D., Bogaerts, S., 2004. From Europe to Africa and vice versa: evidence for multiple intercontinental dispersal in ribbed salamanders (genus *Pleurodeles*). *J. Biogeogr.* 31, 159–171.

- Wake, D.B., Özeti, N., 1969. Evolutionary relationships in the family Salamandridae. *Copeia* 1969, 124–137.
- Weisrock, D.W., Macey, J.R., Ugurtas, I.H., Larson, A., Papenfuss, T.J., 2001. Molecular phylogenetics and historical biogeography among salamandrids of the “true” salamander clade: rapid branching of numerous highly divergent lineages in *Mertensiella luschani* associated with the rise of Anatolia. *Mol. Phylogenet. Evol.* 18, 434–448.
- Weisrock, D.W., Harmon, L.J., Larson, A., 2005. Resolving the deep phylogenetic relationships among salamander families: analyses of mitochondrial and nuclear genomic data. *Syst. Biol.* 54, 758–777.
- Zajc, I., Arntzen, J.W., 1999. Phylogenetic relationships of the European newts (genus *Triturus*) tested with mitochondrial DNA sequence data. *Contrib. Zool.* 68, 73–81.
- Zhao, E., 1998. China Red Data Book of Endangered Animals, Amphibia & Reptilia. Science Press, Beijing, China.